Published in final edited form as:
J Magn Reson Imaging. 2014 June ; 39(6): 1558–1568. doi:10.1002/jmri.24310.

Characterization of thalamocortical association using amplitude and connectivity of fMRI in mild traumatic brain injury

Yongxia Zhou, PhD[1], **Yvonne W Lui, MD**[1], **Xi-Nian Zuo, PhD**[2], **Michael P. Milham, MD, PhD**[3], **Joseph Reaume, BS**[1], **Robert I. Grossman, MD**[1], and **Yulin Ge, MD**[1]

[1]Department of Radiology / Center for Biomedical Imaging, NYU Langone Medical Center, New York, NY 10016

[2]Laboratory for Functional Connectome and Development, Key Laboratory of Behavioral Science, Magnetic Resonance Imaging Research Center, Institute of Psychology, Chinese Academy of Sciences, Beijing, China

[3]Child Mind Institute, New York, NY, United States

Abstract

Purpose—To examine thalamic and cortical injuries using fractional amplitude of low-frequency fluctuations (fALFF) and functional connectivity MRI (fcMRI) based on resting state (RS) and task-related fMRI in patients with mild traumatic brain injury (MTBI).

Materials and Methods—Twenty-seven patients and 27 age-matched controls were recruited. 3T fMRI at RS and finger tapping task were used to assess fALFF and fcMRI patterns. fALFF was computed with filtering (0.01-0.08Hz) and scaling after preprocessing. fcMRI was performed using a standard seed-based correlation method, and delayed fcMRI (coherence) in frequency domain were also performed between thalamus and cortex.

Results—In comparison with controls, MTBI patients exhibited significantly decreased fALFF in the thalamus (and frontal/temporal sub segments) and cortical frontal and temporal lobes; as well as decreased thalamo-thalamo and thalamo-frontal/thalamo-temporal fcMRI at rest based on RS-fMRI (corrected $P<0.05$). This thalamic and cortical disruption also existed at task-related condition in patients.

Conclusion—The decreased fALFF (i.e. lower neuronal activity) in the thalamus and its segments provides additional evidence of thalamic injury in patients with MTBI. Our findings of fALFF and fcMRI changes during motor task and resting state may offer insights into the underlying cause and primary location of disrupted thalamo-cortical networks after MTBI.

Keywords

Fractional amplitude of low frequency fluctuation; functional connectivity (fcMRI); coherence; mild traumatic brain injury; thalamus; resting-state fMRI

Address correspondence and reprint requests to: Dr. Yulin Ge, MD, Center for Biomedical Imaging, Department of Radiology, New York University School of Medicine, 660 First Avenue, 4th floor, New York, NY 10016 USA, yulin.ge@nyumc.org, Phone: (212) 263-3784, Fax: (212) 263-7541.

Following mild traumatic brain injury (MTBI), a substantial number of patients have measurable neuro-cognitive symptoms (1); however, the underlying pathophysiology of post concussive syndrome (PCS) is still poorly understood. Although subsequent brain abnormalities are difficult to detect by conventional MRI imaging, thalamic abnormalities have been detected in MTBI using several advanced neuroimaging techniques such as spectroscopic, perfusion and functional MRI (2-4). Multiple functional thalamic pathways converge on the thalamus, forming a unique architecture to the thalamus, dividing it into clusters of discrete nuclei. Maxwell et al (5) in 2004, using stereological techniques, published a quantitative study revealing evidence of neuronal loss in specific thalamic nuclei (e.g., dorsal medial nucleus [DMN] and ventral posterior nucleus [VPN]) in moderate and severely disabled TBI. It is not known whether thalamic injury is primary or secondary after TBI. Additionally, fewer reports focus on MTBI, which form the majority of TBI cases.

The thalamus has been described as the anatomic threshold to consciousness (6). It is the central relay station of the brain and is also an important and primary generator of brain waves such as alpha (with frequency between 8 to 12 Hz) and gamma waves (with frequency between 25 to 100 Hz). Alpha waves are associated with relaxed awareness in an idle state (7-9). On the other hand, gamma waves are associated with conscious perception and play a role in the interaction and organization of multimodality inputs (e.g. motor and sensory) (10,11). On a cellular level, recent findings on pacemaker neurons suggest that these thalamic spindles could lead to synchronized cortical network oscillations within the gamma band by entraining other cells with their firing patterns (9). One of the suggested mechanisms for conscious attention of the gamma wave originating in the thalamus and its importance for conscious awareness under coma situation had been proposed by Pollack (12). He goes on to say that “If the thalamus was damaged even a little bit”, such as in traumatic episode case, “the gamma wave stops, conscious awarenesses do not form, and the patient slips into profound coma”. Likewise, if the coupling between the thalamus and other brain structures is hindered, the impact of arousal related processes on cerebral responses may become impaired (13,14).

Recently investigators have been able to localize these waves in the brain using resting state (RS)-fMRI (15,16). Cortical gamma oscillation is often difficult to localize due to higher temporal resolution requirement and higher synchrony of brain status. The GABA concentration measured with in vivo MR spectroscopy had recently found to be able to predict gamma activity measured with task-related EEG and fMRI in the visual cortex (17). Despite the important role of the thalamus in conscious awareness, no direct measurements of brain oscillation networks based on both RS-fMRI and task-related fMRI have been applied in MTBI patients.

Functional connectivity MR imaging (fcMRI) based on fMRI measures the synchronous correlation (traditionally instantaneous analysis) between two designated regions (i.e. seed and target) in the brain (18). Using RS-fMRI, our previous work has documented disrupted default mode network fcMRI (4) and abnormal thalamo-cortical connectivity (19) in patients with MTBI. However, connectivity with delayed response of two connected regions (so called non-zero time lag) is not addressed by conventional fcMRI, though can be detected using coherence in the frequency domain (20). Of particular interest to this study are

thalamocortical connections involving frontal, temporal, primary motor and sensory cortical regions which are known to be time-delayed. Besides using fcMRI for measuring functional connectivity, intrinsic neuronal activity within a specific brain region (or even expanding to the whole brain) needs to be further quantified to better understand origin of the alterations in fcMRI (i.e. whether such changes are attributable to changes in intrinsic neuronal activity of the seed or target region or connectivity changes between the seed and target).

The fALFF method was first developed by Zang et al and had been found to be a robust and rigid marker to detect spontaneous neuronal activity (21) based on RS-fMRI data. For example, in the resting state, fALFF has been shown to be higher in the default mode network (DMN) regions that are active (22) and to be altered in various disease states (21,23,24). The stability and test-retest reliability of the fALFF measure has also been addressed and results show a reliable pattern in either resting-state or task-related conditions (25). Furthermore, several studies have also demonstrated task-related (e.g. working memory, motor visual stimuli and cognitive tasks) alterations of low-frequency oscillations that are believed to reflect real-time neuronal activity (26-28).

We hypothesize that there is local thalamic injury after MTBI which affects functional interactions between the thalamus and cortex. We aim to: 1) examine fALFF, a neuronal activity marker, to detect thalamic and/or cortical injury in MTBI based on a well-defined thalamic segmental template and whole brain voxel-wise technique with both RS-fMRI and finger tapping task-related fMRI; 2) demonstrate thalamo-thalamo and thalamo-cortical instantaneous fcMRI changes with both RS-fMRI and task-related fMRI seeding from the entire thalamus as well as its segments; 3) investigate differences between MTBI subjects and controls in delayed thalamo-cortical fcMRI using coherence in the frequency domain.

Materials and Methods

Participants and neuropsychological tests

Twenty-seven patients (mean age of 33.4 ±std 11.2 years; 6 female and 21 males) and 27 demographically similar healthy controls (mean age of 35.4 ± STD 11.4 years; 13 female and 14 males) were involved in this study. Our institutional review board approved this study, and written informed consent forms of all study subjects were obtained after the nature of this study was explained to the subjects prior to participation. The mean interval between MRI and trauma for patients was 23 days (range: 3-58 days); and the mean loss of consciousness duration was 12 minutes (range: 1-30 minutes). All patients were recruited from a level one trauma center and sustained MTBI defined by clinical criteria (1) including Glasgow Coma Scale (GCS) between 13 and15, and had various post-traumatic symptoms. The injury mechanisms of patients including 8 motor vehicle accident, 7 assault, 6 falls, 3 sports related, 2 bicycle collisions, 1 others) and location of injury include 3 on the left side, 9 on the right side, 5 on the back, 2 on the forehead, 8 of other regions of the brain.

Neuropsychological tests (including 6 types of neuropsychological tests and PCS clinical measure) were performed within 24 hours of the MRI scan for each subject. Posttraumatic symptoms including anxiety, depression, and fatigue were assessed using self-report

questionnaires and scales, for which higher scores indicate greater symptomatology. MTBI patients showed significantly increased PCS scores compared to controls (P = 0.003).

MRI Imaging

MRI data were obtained at 3T whole-body MR scanner (Siemens Tim Trio, Erlangen, Germany) using a 12-channel head coil. Standard gradient-echo echo-planar imaging (EPI) based RS-fMRI (TR/TE=2000/30msec, flip angle=75°, field of view (FOV)=220x220mm^2, matrix=128×128, 153 volumes) was performed with an acquisition time of 5 minutes and 6 seconds. A total of 20 slices with thickness of 5mm and 1 mm gap was positioned parallel to the AC-PC line and to cover the entire cerebrum (spatial resolution, 1.72×1.72×6.00 mm^3). Subjects were instructed to close their eyes and relax, but remain awake during the RS-fMRI imaging. For coregistration and normalization of RS-fMRI data, three-dimensional T1-weighted magnetization-prepared rapid gradient-echo (MPRAGE) images (TR/TE/TI=2300/2.98/900ms, flip angle=9°, resolution=1×1×1mm^3) were obtained. The conventional T1- and T2-weighted together with susceptibility weighted imaging (SWI) images, as previously described (4,19), were carefully reviewed by two experienced radiologists, and lesions, if present, were documented.

We then examined the fALFF and fcMRI at active status to better understand the fMRI signal changes at both signal and frequency domains. This was done by implementing a task-related paradigm inside the scanner: a finger-tapping task-related EPI based fMRI scans (30 seconds of index finger movement at regular pace with left hand alternating with 30 seconds at rest; with a total of 5 repetitions for each condition). Out of the total subjects, 7 patients and 8 controls performed finger-tapping task-related scans. The parameters for the task-related fMRI sequence are set to the same as the RS-fMRI (TR/TE=2000/30msec, flip angle=75°, FOV=220×220mm^2). The finger tapping started at 6 seconds after scans with a total of 153 volumes. Subjects received instruction on testing procedures prior to the MRI scan and were signaled by screens projecting visual cues for tapping and not-tapping task during scans.

Image Processing and Data Analysis

Preprocessing—Anatomical and functional data (both resting state and task conditions) were preprocessed using both FSL (http://www.fmrib.ox.ac.uk/fsl) and AFNI (adapted scripts from http://www.nitrc.org/projects/fcon_1000). Preprocessing steps of fMRI data included sequentially, realignment, spatial Gaussian smoothing with full width at half maximum (FWHM) =6mm, band pass temporal filtering 0.01-0.08 Hz as used most widely, using regression model to remove nuisance signals (ie. six motion parameters, signals derived from cerebrospinal fluid and white matter masks after segmentation as well as global signal), coregistration to anatomical MPRAGE data, and transformation to MNI152 space (2×2×2mm^3) with the nonlinear optimization warping algorithm called FMRIB's Non-linear Image Registration Tool (FNIRT, http://www.fmrib.ox.ac.uk//fsl). For motion artifact correction, a head movement-constraint headphone and cushion were used and more software-based realignment steps were performed with six motion parameter to further minimize the motion artifacts (4).

fALFF Calculation—The idea of fALFF method was to scale the summary of amplitude across the low-frequency band (e.g. 0.01-0.08Hz) to the summary of amplitude across whole band in the frequency domain to remove white and physiological noise (21). The amplitude of low frequency fluctuation (ALFF) calculated from RS-fMRI initially suggested to reflect the intensity of regional spontaneous brain activity at rest, and furthermore fALFF showed higher sensitivity and specificity than ALFF with less contamination from vascular signals. In this study, after despiking, detrending, spatial smoothing (FWHM=6mm) and global mean scaling based on AFNI commands to the pre-filtered time course (only realignment preprocessing step applied to the original time course), the whole-brain voxel-wise fALFF was calculated for each voxel using FSL *fslpspec* function of either resting state or task-related fMRI data according to equation [1] (25). The fALFF value of each voxel was first z-standardized across whole brain to obtain the z-score value by subtracting the whole-brain mean and divided by standard deviation, and then warped into the MNI152 space for group analysis using the transformation matrix from the preprocessing step.

$$fALFF_x = \frac{\sqrt{\sum_{k\in[0.01,0.08]} |P_{xx}(k)|^2}}{\sqrt{\sum_{k\in[0,N/(2N+1)\bullet 1/T_s]} |P_{xx}(k)|^2}}, T_s = 2sec, N = 150 \quad [1]$$

where Pxx(k) is the power spectrum function of time course x(t) of a voxel in frequency domain.

Thalamic Seed-based fcMRI—fcMRI (29) of both resting state and task conditions between two time series of the seed and each voxel over the whole brain was computed after standard pre-processing steps outlined earlier (ie. realignment, smoothing, band-pass filtering, regression out nuisance parameters and normalization applied sequentially), with equation [2].

$$\rho_{xy} = \frac{\sum_{i=1}^{N}(X_i - \overline{X}) \cdot (Y_i - \overline{Y})}{\sqrt{\sum_{i=1}^{N}(X_i - \overline{X})^2} \cdot \sqrt{\sum_{i=1}^{N}(Y_i - \overline{Y})^2}}, \quad N = 150 \quad [2]$$

where X(t) and Y(t), t=1,…,N are time courses of two voxels.

In our study, to further investigate the thalamo-cortical fcMRI, the seed was placed over the entire bilateral thalamus as well as within seven thalamic subfields (7 segments total from the FSL template based on diffusion data demonstrated in Figure 3B) for computing the Pearson's correlation between the preprocessed average time series of the seed and each voxel (including thalamic area itself) within the whole brain area. The resultant Rho values were z-transformed with Fisher's r-to-z transformation and were used for subsequent group-level analysis.

Thalamo-cortical Coherence Computation—To analyze the delayed (all time-lag) thalamo-thalamo or thalamo-cortical connectivity (or synchronization), temporal coherence (20) was computed based on the cross-correlation between average time courses of the voxels from left and right thalamus (thalamo-thalamo) as well as the cross-correlation between average time courses of the voxels from the entire bilateral thalamus and each of 44 cortical Brodmann Areas (BAs) (thalamo-cortical) using in-house Matlab (www.mathworks.com) scripts according to equation [3].

$$C_{xy}(k)=\frac{|P_{xy}(k)|^2}{|P_{xx}(k)\cdot P_{yy}(k)|},\quad P_{xx}(k)=\left|FFT\left\{X(t)\cdot\ X(t)\right\}\right|,\quad P_{xy}(k)=\left|FFT\left\{\frac{r_{xy}(t)}{\sigma_x\sigma_y}\right\}\right| \quad [3]$$

$$\textit{where}\ r_{xy}(t)=E[(x_\tau-\mu_x)\cdot(y_{\tau+t}-\mu_y)],\quad k=(0,\cdots,N)\cdot\frac{1}{T_s\cdot(2\mathrm{N}+1)},\quad T_s=2\mathrm{sec},\quad N=150$$

X(t) and Y(t) are two time series of two voxels; σ_x and σ_y are the standard deviation of X(t) and Y(t) respectively to normalize the cross-correlation (r_{xy}) between X and Y; Pxx(k) is the power spectrum function of time course x(t) of a voxel; and Pxy(k) is the cross-power spectrum of the cross-correlation between two time courses X(t) and Y(t).

Statistical Analysis

For group-level motion correction, after preprocessing steps of regression out six motion parameters, statistical comparison using two-sample t-test of the six motion parameters including three angular rotations (roll, pitch, and yaw in units of degrees) and three directional displacement (in millimeters) and dynamic frame displacement (summary of all six parameters in millimeters) (30) along all temporal frames were implemented between MTBI and control groups to test if any differences of motion parameters.

For comparison of fALFF or fcMRI between RS and task-related conditions, 1 sample paired t-test for the matched-pairs sample of repeated fMRI measures done at RS and task was used within each separate patient and control group. In addition, two-sample t-test was used to compare fALFF or fcMRI maps between patients and controls. A ROI-based average was also performed on the seven sub-segments of thalamic diffusion projection FSL template, in order to investigate the segmental alterations of fALFF in patients compared to controls for RS-fMRI. For both fALFF and fcMRI analyses, multiple-comparison corrections at whole brain level were performed with 1-sample paired t-test: an integrated threshold was used with a significant level for small volume correction to the whole brain in order to remove false positive error and maintain true positive sensitivity that were reported respectively (31). Empirical $P<0.05$ and cluster size $K>20$ were applied to fALFF results; and $P<0.001$ and $K\geq100$ were applied to fcMRI results after using a 25% gray matter mask from the FSL standard template

Multiple comparison corrections at the cluster level were also performed to the whole brain to the statistical results of fALFF and fcMRI obtained with 2-sample t-test based on Gaussian random field (GRF) theory using FSL *easythresh* (minimum $Z>2.3$; cluster significance, $P<0.05$, corrected).

Results

To better understand the synchronized low-frequency spontaneous fluctuations of fMRI signal between thalamus and cortex, we have evaluated the fMRI signal amplitude changes over time and power spectrum on frequency domain during rest and when finger-tapping task was performed in each of these two regions. As shown in Figure 1, when the ROI was placed in the motor cortex (Figure 1A) in a normal control, a significant increase of fMRI difference signal was seen between task and control conditions during motor task time course as compared to resting state acquisition (Figure 1B), while the power spectrum (Figure 1C) showed significant increase of fALFF during the task at relatively low frequency band (0.01~0.08 Hz). When the ROI was placed in the thalamus (Figure 1D), there was consistent increase of BOLD signal during motor task than resting state (Figure 1E) and slight increase of fALFF on power spectrum between task and resting state (Figure 1F).

Regarding motion artifact correction, we found very similar head motion of the six realignment parameters and frame displacement between MTBI and control groups ($P>0.05$). Group analysis showed significant increase of fALFF in the thalamus, motor and supplementary motor areas during finger-tapping compared to resting state (Figure 2A) (one-sample paired t-test, $P<0.05$, $K>20$) in the control subjects. There was also decreased fALFF in the default-mode areas (eg. posterior cingulate) in the control subjects and the activation of default mode network were suppressed under task-condition as expected ($P<0.05$, $K>20$). In MTBI patients, fALFF difference map between finger-tapping and resting state RS-fMRI showed less fALFF change in the thalamus and primary motor areas and less de-activation of default mode network areas when compared to controls ($P<0.05$, $K>20$) (Figure 2B).

Based on RS-fMRI data, whole brain voxel-based analysis showed that patients demonstrated significantly reduced fALFF in regions including frontal, temporal, and occipital cortices (Figure 3A) compared to controls (minimum $Z>2.3$; cluster significance, $P<0.05$, corrected). More specifically, there was significant reduction fALFF in the entire bilateral thalamus ($P=0.004$) (Figure 3B), as well as thalamic segments projecting to frontal (FSL thalamic template index 4) ($P=0.012$), temporal (FSL thalamic template index 7) ($P=0.015$) and occipital cortices (FSL thalamic template index 3) ($P=0.027$), in MTBI patients compared to controls (Figure 3C).

Regarding functional connectivity measured with fcMRI, there was significantly reduced thalamo-thalamo fcMRI seeding from the thalamus (Figure 4 A), as well as seeding from its segments for frontal (segment 4) (Figure 4B) and temporal (FSL segment7) (Figure 4C) projections compared to controls (corrected $P<0.05$) based on RS-fMRI. There was also decreased thalamo-cortical fcMRI in the frontal and temporal regions in the MTBI patients compared to controls; with increases of fcMRI in the occipital and parietal regions (including scattered frontal white matter regions). The detailed comparison results between two groups seeding from two thalamic sub-segments were listed in Table 1 (from segment 4) and Table 2 (from segment 7). The common and different findings of fALFF and fcMRI based on RS-fMRI are summarized in Table 3 for thalamo-thalamo measurements and Table

4 for thalamo-cortical measurements. With task-related fMRI data using the same fcMRI method, we found that in healthy controls the thalamo-cortical network (with seeding from the entire thalamus) showed significantly increased fcMRI in the supplementary and primary motor cortices during finger tapping compared with resting state using a paired t-test (minimum $Z>2.3$; cluster significance, $P<0.05$, corrected; cluster size $K\geq 20$ in Figure 5 A), which were consistent with fALFF findings (Figure 2). In MTBI patients, however, group-wise results of comparison showed decrease or lack of thalamo-motor connectivity during finger tapping task as compared to resting state (Figure 5B, corrected $P<0.05$)

Using coherence to the RS-fMRI, we found that the strong thalamo-cortical coherence was predominantly in the low-frequency range (0.01-0.08Hz) with maximal value of 0.45 in controls increased to 0.53 in MTBI patients (~18% increment). There was also increased coherence between thalamus and almost all cortical BA regions predominantly in the low frequency band ($P<0.05$) (Figure 6A). Moreover, there was a positive correlation between low-frequency thalamo-cortical coherence averaged across all cortical BA regions over low-frequency band and PCS score in MTBI patients (Spearman rank $r=0.4$, $P=0.029$) (Figure 6B).

Discussion

We found significantly reduced fALFF in the whole thalamus and particularly in the thalamic subregions projecting to frontal and temporal projected cortex (segments 4 and 7 respectively), indicating decreased spontaneous thalamic neuronal activity believed to be a result of subtle injury in these patients. Notably, no focal abnormalities were observed in the thalami on conventional structural imaging. There was also decreased frontal and temporal cortical fALFF in patients compared to controls at resting-state, further supporting the notion that the frontal and temporal regions themselves are abnormal as well after MTBI. In addition, we found the thalamo-thalamo, thalamo-temporal and thalamo-frontal connectivity (fcMRI), with seeding from thalamic segments 4 and 7, to be reduced in MTBI patients compared to controls. The decreased thalamo-frontal and thalamo-temporal fcMRI, and fALFF reduction co-validates that these areas may be more predisposed to injury (1). It is known that the frontal and temporal lobes are at increased risk of contusion in moderate and severe injury. Hypometabolism in the thalamus, frontal and temporal lobes had also been reported in severe TBI patients based on PET FDG uptake imaging (32). Our results of abnormal fALFF and fcMRI indicate that the thalamo-cortical network is disrupted in patients shortly after MTBI both in strength and in spatial extent and these changes may be neuropychological origins of PCS in these patients.

At finger tapping task condition, we found that in controls, as expected, the increased fALFF at motor and supplemental motor cortex were co-localized with the increased neuronal activation sites during the finger-tapping task. This task-related regional increased fALFF, together with our findings in the thalamus further confirm that fALFF reflects neuronal activity. Experimental study of thalamocortical circuits of the rat somatosensory system showed that the synchronous thalamic firing is produced and strongly engaged in cortical neuronal activity that is associated with sensorimotor stimuli (33). The fcMRI between the thalamus and co-activated motor/supplementary motor regions during finger tapping task

compared to resting state was also increased in controls, suggesting a normal functional response with increased synchronicity between these two regions induced by neuronal stimuli or tasks. In contrast, patients with MTBI failed to show such expected task-related upregulation measured with fALFF and fcMRI. These findings support the hypothesis of disengagement of resting or “idling” brain baseline condition in these patients with MTBI (4).

In the resting state, one important function of the thalamic reticular nuclei is inhibition. These nuclei have rich GABAergic neurons which act as inhibitory intermediaries not only within thalamic nuclei but also for longer-range thalamocortical interaction (34,35). Along with abnormal thalamic activation during task, the current study also showed significantly reduced fALFF in the thalamus, predominantly in segments 3, 4 and 7, in MTBI patients as compared with healthy controls. Correspondingly, we also found disrupted thalamo-cortical connectivity and reduced thalamo-thalamo fcMRI in patients with the most abnormal patterns within segments 4 and 7. Segments 4 and 7 represent the medial frontal and medial dorsal subdivisions of the thalamus, which relay inputs from the amygadala and project to the prefrontal cortex and the limbic system. As a result, these nuclei in particular play a crucial role in attention, planning, organization, abstract thinking, and active memory, domains in which patients with MTBI often have deficits. Our findings of reduced thalamic fALFF in patients corroborate with the previous notion that the thalamus is injured after MTBI and furthermore reduced fALFF suggest that this thalamic injury may be the primary cause of significantly disrupted thalamocortical functional connectivity as observed in this study and a previous study (19). The thalamic subfields defined with FSL template may serve as a functional atlas for localizing areas of the thalamus that improve the specificity of thalamic injury. Our fcMRI results better localize thalamic connectivity alterations with some regions of increased and other regions of decreased connectivity in MTBI patients as compared with controls, while only increased thalamocortical fcMRI was found in MTBI in a previous study (19). The difference in fcMRI results may be explained by the fact that different pre-processing steps were used: the previous study examined connectivity with seeding of the entire thalamus without low-pass filtering and used a single-subject template, and the current study employs both positive and negative connectivity with seeding of thalamic subfields based on a more general averaged template. In particular, we found increased thalamo-occipital fcMRI in MTBI patients compared to controls, but, of note, we also saw decreased occipital fALFF in these patients. Negative thalamo-occipital connectivity in the resting-state fMRI has been previously reported in controls (17). This leads us to speculate that there is a reduction in the normal negative thalamo-occipital connectivity after MTBI, resulting in the observed increase in fcMRI in patients.

Moreover, compared to controls, there was consistently higher thalamo-cortical coherence at the low-frequency band despite the reductions of fALFF and fcMRI in the thalamus and frontal/temporal cortical regions that were found in MTBI patients. Coherence, a regional homogeneity measure for synchronization in frequency domain, was found to be insensitive to phase variability across the measured time series (36). One possible explanation is that the input and output of different neuronal networks involving the thalamus and frontal/temporal regions might undergo temporally distortion due to injury effecting the network organization, thereby increasing coherence, a reflection of both instantaneous and delayed

connectivity, but decreasing instantaneous connectivity and neuronal activity. Differences and similarities between conventional fcMRI and coherence results had been previously reported in controls (37) as well as various brain disorders (38). This again may indicate that at resting state in the normal brain, the thalamocortical functional networks are only loosely connected, while in MTBI, different components of the thalamic oscillator (e.g. alpha and gamma waves, thalamic GABAergic neuron disinhibition) shift away from a stable lower-energy state and result in increased thalamic-cortical synchrony. A possible underlying mechanism is that thalamic neurons, when injured, fire with less frequency but are more coherent with cortical regions. Alternatively, there is a possibility that external signals (e.g. cortical frontal or temporal damage) induce the transition from a decoherent state to a more coherent state under which bursts of thalamic neurons occur more simultaneously. Furthermore, this abnormal increased coherence correlated with severity of post-traumatic symptoms, suggesting that the increased coherence may influence the degree or severity of the post-traumatic symptoms in MTBI patients as a response to trauma.

Consistent and complementary results of fcMRI and fALFF at resting state and task conditions in controls had been reported before (39). Our results of the reduced fALFF and fcMRI in the thalamus and between the thalamus and frontal/temporal regions in patients suggest that the thalamo-thalamo and thalamo-cortical network disruption were reflected not only at slow-pace resting state, but also during real-time active state. Thalamic injury and thalamo-cortical response in MTBI have not been well appreciated due to the lack of sensitive techniques that can detect the subtle damage in vivo. Results of systematic characterization of thalamocortical activity and connectivity may have important therapeutic implications in these patients as underscored by a recent report (40) in which a patient, who had been in a minimally conscious state for many years following traumatic brain injury, showed dramatic improvement with thalamic stimulation. One of the limitations of the current work is that the thalamic segmentation was derived from a common FSL structural atlas. A more precise delineation of thalamic nuclei based on full-spectrum features including partial correlations between fMRI time courses will improve the segmental fcMRI and fALFF quantification results.

In conclusion, we have shown consistent decreased thalamic and frontal/temporal fALFF and decreased thalamo-thalamo fcMRI both at resting state and at task conditions, especially involving segments with frontal and temporal projections. Abnormally increased thalamo-cortical coherence in the low-frequency band which correlated with clinical status has also been demonstrated. Our results support the concept that specific thalamic and cortical regions are involved in injury after MTBI and these may play a crucial role in the pathomechanisms of post concussive syndrome in these patients.

References

1. Silver, JM.; McAllister, TW.; Yudofsky, SC. Textbook of Traumatic Brain Injury. 2. American Psychiatric Publishing, Inc; 2011.
2. Ge Y, Patel MB, Chen Q, et al. Assessment of thalamic perfusion in patients with mild traumatic brain injury by true FISP arterial spin labelling MR imaging at 3T. Brain Inj. 2009; 23(7):666–674. [PubMed: 19557570]

3. Kirov I, Fleysher L, Babb JS, Silver JM, Grossman RI, Gonen O. Characterizing 'mild' in traumatic brain injury with proton MR spectroscopy in the thalamus: Initial findings. Brain Inj. 2007; 21(11): 1147–1154. [PubMed: 17882630]
4. Zhou Y, Milham MP, Lui YW, et al. Default-mode network disruption in mild traumatic brain injury. Radiology. 2012; 265(3):882–892. [PubMed: 23175546]
5. Maxwell WL, Pennington K, MacKinnon MA, et al. Differential responses in three thalamic nuclei in moderately disabled, severely disabled and vegetative patients after blunt head injury. Brain. 2004; 127(Pt 11):2470–2478. [PubMed: 15456707]
6. Jones, EJ. The Thalamus. 2. Vol. 2. Cambridge University Press; 2007.
7. Chatila M, Milleret C, Rougeul A, Buser P. Alpha rhythm in the cat thalamus. C R Acad Sci III. 1993; 316(1):51–58. [PubMed: 8495387]
8. Lopes da Silva FH, Hoeks A, Smits H, Zetterberg LH. Model of brain rhythmic activity. The alpha-rhythm of the thalamus. Kybernetik. 1974; 15(1):27–37. [PubMed: 4853232]
9. Schreckenberger M, Lange-Asschenfeldt C, Lochmann M, et al. The thalamus as the generator and modulator of EEG alpha rhythm: a combined PET/EEG study with lorazepam challenge in humans. Neuroimage. 2004; 22(2):637–644. [PubMed: 15193592]
10. Buzsaki G, Wang XJ. Mechanisms of gamma oscillations. Annu Rev Neurosci. 2012; 35:203–225. [PubMed: 22443509]
11. Engel AK, Fries P, Konig P, Brecht M, Singer W. Temporal binding, binocular rivalry, and consciousness. Conscious Cogn. 1999; 8(2):128–151. [PubMed: 10447995]
12. Pollack, R. The Missing Moment: How the Unconscious Shapes Modern Science. Houghton Mifflin; 1999.
13. Kempf F, Brucke C, Salih F, et al. Gamma activity and reactivity in human thalamic local field potentials. Eur J Neurosci. 2009; 29(5):943–953. [PubMed: 19291224]
14. Sun Y, Farzan F, Barr MS, et al. gamma oscillations in schizophrenia: mechanisms and clinical significance. Brain Res. 2011; 1413:98–114. [PubMed: 21840506]
15. Ben-Simon E, Podlipsky I, Arieli A, Zhdanov A, Hendler T. Never resting brain: simultaneous representation of two alpha related processes in humans. PLoS One. 2008; 3(12):e3984. [PubMed: 19096714]
16. Zou Q, Long X, Zuo X, et al. Functional connectivity between the thalamus and visual cortex under eyes closed and eyes open conditions: a resting-state fMRI study. Hum Brain Mapp. 2009; 30(9):3066–3078. [PubMed: 19172624]
17. Muthukumaraswamy SD, Edden RA, Jones DK, Swettenham JB, Singh KD. Resting GABA concentration predicts peak gamma frequency and fMRI amplitude in response to visual stimulation in humans. Proc Natl Acad Sci U S A. 2009; 106(20):8356–8361. [PubMed: 19416820]
18. Haacke EM, Duhaime AC, Gean AD, et al. Common data elements in radiologic imaging of traumatic brain injury. J Magn Reson Imaging. 2010; 32(3):516–543. [PubMed: 20815050]
19. Tang L, Ge Y, Sodickson DK, et al. Thalamic resting-state functional networks: disruption in patients with mild traumatic brain injury. Radiology. 2011; 260(3):831–840. [PubMed: 21775670]
20. Sun FT, Miller LM, D'Esposito M. Measuring interregional functional connectivity using coherence and partial coherence analyses of fMRI data. Neuroimage. 2004; 21(2):647–658. [PubMed: 14980567]
21. Zang YF, He Y, Zhu CZ, et al. Altered baseline brain activity in children with ADHD revealed by resting-state functional MRI. Brain Dev. 2007; 29(2):83–91. [PubMed: 16919409]
22. Zou QH, Zhu CZ, Yang Y, et al. An improved approach to detection of amplitude of low-frequency fluctuation (ALFF) for resting-state fMRI: fractional ALFF. J Neurosci Methods. 2008; 172(1):137–141. [PubMed: 18501969]
23. Hoptman MJ, Zuo XN, Butler PD, et al. Amplitude of low-frequency oscillations in schizophrenia: a resting state fMRI study. Schizophr Res. 2010; 117(1):13–20. [PubMed: 19854028]
24. Zhang G, Yin H, Zhou YL, et al. Capturing amplitude changes of low-frequency fluctuations in functional magnetic resonance imaging signal: a pilot acupuncture study on NeiGuan (PC6). J Altern Complement Med. 2012; 18(4):387–393. [PubMed: 22515798]

25. Zuo XN, Di Martino A, Kelly C, et al. The oscillating brain: complex and reliable. Neuroimage. 2010; 49(2):1432–1445. [PubMed: 19782143]
26. Bajo R, Maestu F, Nevado A, et al. Functional connectivity in mild cognitive impairment during a memory task: implications for the disconnection hypothesis. J Alzheimers Dis. 2010; 22(1):183–193. [PubMed: 20847450]
27. Duff EP, Johnston LA, Xiong J, Fox PT, Mareels I, Egan GF. The power of spectral density analysis for mapping endogenous BOLD signal fluctuations. Hum Brain Mapp. 2008; 29(7):778–790. [PubMed: 18454458]
28. Sparing R, Meister IG, Wienemann M, Buelte D, Staedtgen M, Boroojerdi B. Task-dependent modulation of functional connectivity between hand motor cortices and neuronal networks underlying language and music: a transcranial magnetic stimulation study in humans. Eur J Neurosci. 2007; 25(1):319–323. [PubMed: 17241293]
29. Biswal BB. Resting state fMRI: A personal history. Neuroimage. 2012; 62(2):938–944. [PubMed: 22326802]
30. Power JD, Barnes KA, Snyder AZ, Schlaggar BL, Petersen SE. Spurious but systematic correlations in functional connectivity MRI networks arise from subject motion. Neuroimage. 2012; 59(3):2142–2154. [PubMed: 22019881]
31. Bennett CM, Wolford GL, Miller MB. The principled control of false positives in neuroimaging. Soc Cogn Affect Neurosci. 2009; 4(4):417–422. [PubMed: 20042432]
32. Garcia-Panach J, Lull N, Lull JJ, et al. A voxe-based analysis of FDG-PET in traumatic brain injury: regional metabolism and relationship between the thalamus and cortical areas. Journal of Neurotrauma. 2011; 28:1707–1717. [PubMed: 21770759]
33. Shim WH, Baek K, Kim JK, et al. Frequency distribution of causal connectivity in rat sensorimotor network: resting-state fMRI analyses. J Neurophysiol. 2013; 109(1):238–248. [PubMed: 23019001]
34. Aron AR, Schlaghecken F, Fletcher PC, et al. Inhibition of subliminally primed responses is mediated by the caudate and thalamus: evidence from functional MRI and Huntington's disease. Brain. 2003; 126(Pt 3):713–723. [PubMed: 12566291]
35. Steriade M. Sleep, epilepsy and thalamic reticular inhibitory neurons. Trends Neurosci. 2005; 28(6):317–324. [PubMed: 15927688]
36. Saad ZS, Ropella KM, Cox RW, DeYoe EA. Analysis and use of FMRI response delays. Hum Brain Mapp. 2001; 13(2):74–93. [PubMed: 11346887]
37. Muller K, Lohmann G, Neumann J, Grigutsch M, Mildner T, von Cramon DY. Investigating the wavelet coherence phase of the BOLD signal. J Magn Reson Imaging. 2004; 20(1):145–152. [PubMed: 15221820]
38. Salomon RM, Karageorgiou J, Dietrich MS, et al. MDMA (Ecstasy) association with impaired fMRI BOLD thalamic coherence and functional connectivity. Drug Alcohol Depend. 2012; 120(1-3):41–47. [PubMed: 21807471]
39. Kalcher K, Boubela RN, Huf W, et al. RESCALE: Voxel-specific task-fMRI scaling using resting state fluctuation amplitude. Neuroimage. 2012; 70C:80–88. [PubMed: 23266702]
40. Schiff ND, Giacino JT, Kalmar K, et al. Behavioural improvements with thalamic stimulation after severe traumatic brain injury. Nature. 2007; 448(7153):600–603. [PubMed: 17671503]

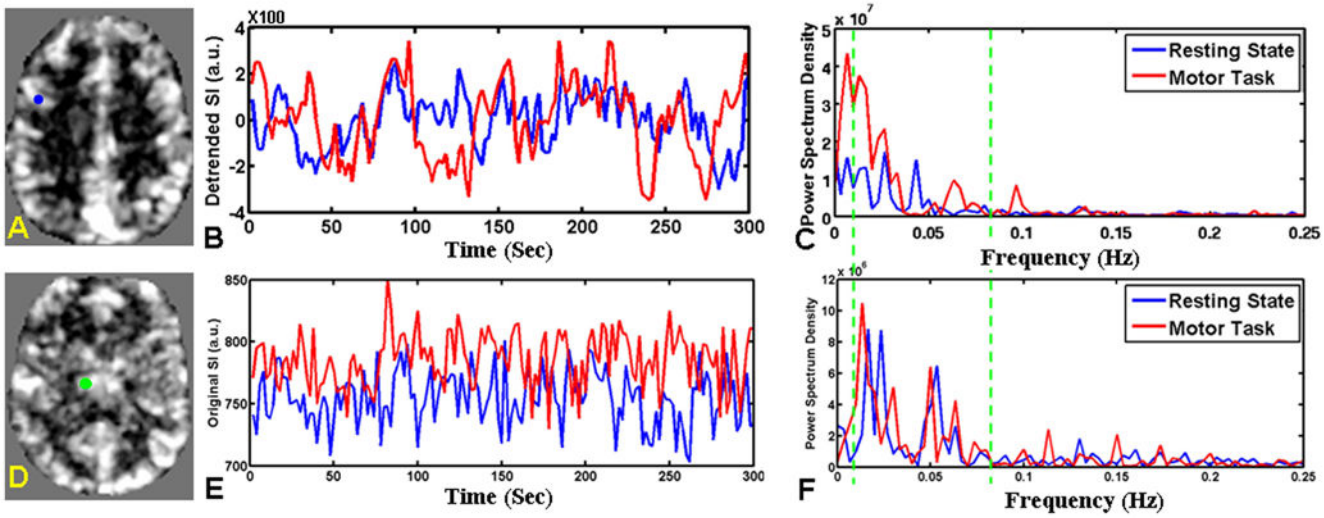

Figure 1.

fALFF features including signal amplitude and power spectrum on frequency domain measured in resting-state and index finger-tapping task with dominant hand conditions in two representative regions of motor cortex and thalamus of a control subject. A: Demonstration of fALFF map at resting state with motor region as ROI in blue color. B: The preprocessed time course of voxels in motor region at the resting state (blue color) and task condition (red color). Compared to resting state, the task-related time course showed increased difference signal between finger tapping condition and control condition across 5 cycles. C: the power spectrum showed increased fALFF (sum of square root of power spectrum at green band over the sum of square root of power spectrum of all frequencies) from the resting state (blue color) to the task condition (red color) with green line showing the low frequency (0.01 Hz) and high frequency (0.08 Hz) cut-off. D showed slice of fALFF map containing thalamus (marked in green color) at resting state; with the time courses and power spectrums showed in E and F. There was slightly increase of fALFF in the thalamus at task condition; but not as great as in the task-related motor region shown in A.

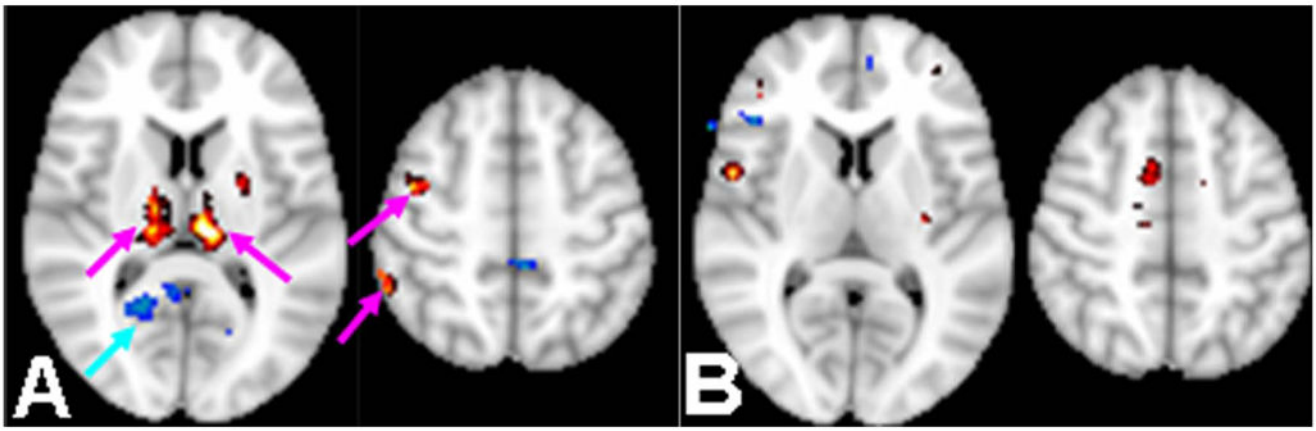

Figure 2.

A: In 8 controls that performed task-related fMRI, difference of fALFF map between finger-tapping condition compared with resting state condition: increased fALFF in the thalamus, motor and supplementary motor areas (red color) as well as thalamus (paired t-test, $P<0.05$, cluster size $K>20$). There was decreased fALFF in the posterior cingulate as part of default-mode areas (blue-color) which were suppressed under task-condition as expected. B: In 7-MTBI patients difference of fALFF map at finger-tapping task condition compared with resting state (RS) condition. Patients showed less co-activation in the thalamus and motor task-related areas (pink arrows in A); and less de-activation of the default-mode network (cyan arrow in A).

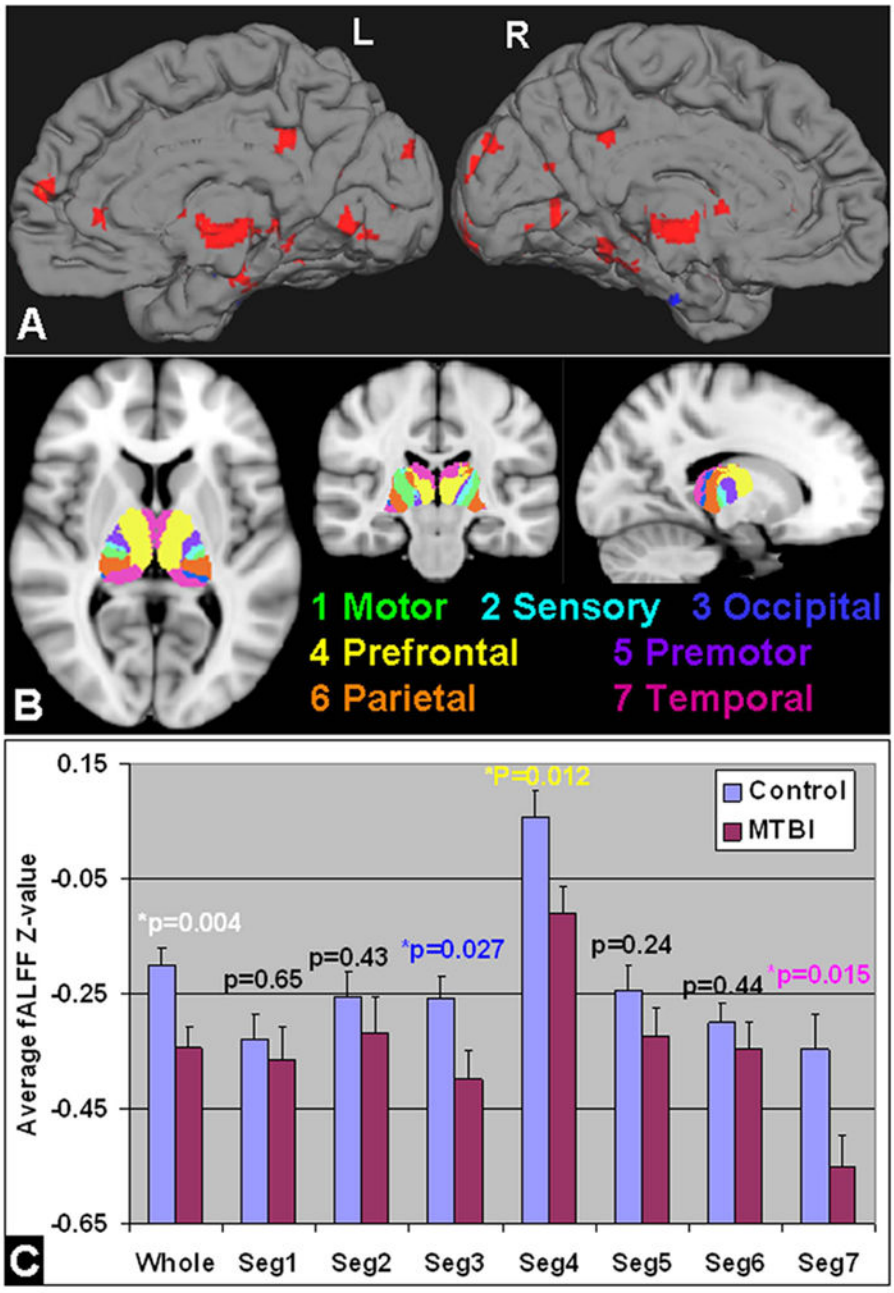

Figure 3.

A: fALFF analysis based on RS-fMRI comparing MTBI with controls in the whole brain showed mostly reduced fALFF in the thalamus, medial frontal, occipital and temporal regions (red color) (minimum Z>2.3; cluster significance, P<0.05, corrected). Results were showed in the medial surface projection views on the left and right hemispheres. Specifically, in the seven thalamic segments according to FSL template (B): there was significantly reduced fALFF in the overall thalamus and its segments for occipital (template index number 3), frontal (4) and temporal (7) projections in MTBI patients compared with

controls ($P<0.05$) (C). As the fALFF was z-standardized over the whole brain; the negative values indicated the thalamic fALFF was less than the whole brain average.

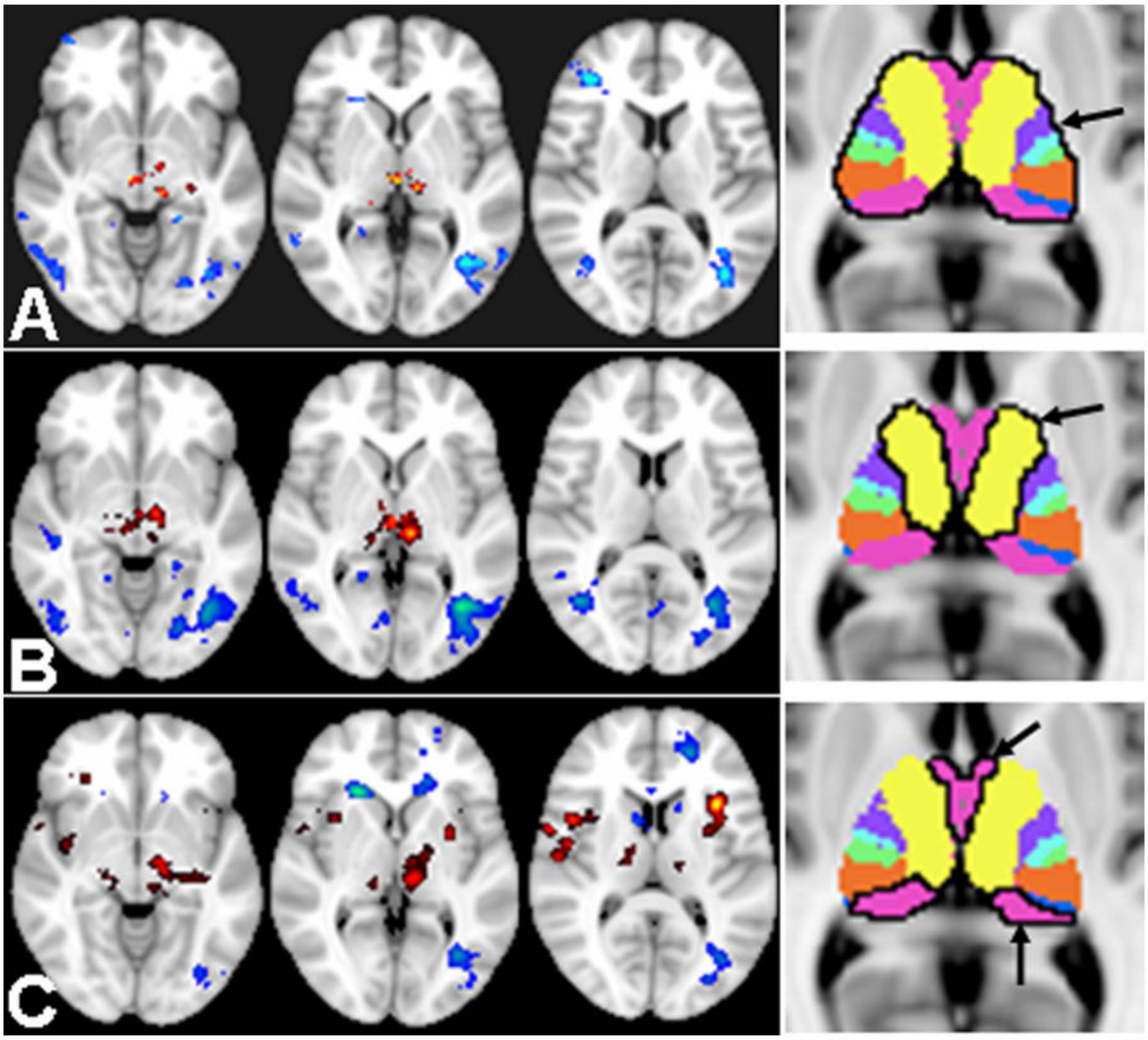

Figure 4.

Based on RS-fMRI, selected slices covering thalamic regions compared fcMRI of MTBI and controls; seeding from bilateral thalamus and its segments (i.e. 4 and 7) marked with black margin on the rightmost images. A: RS-fcMRI seeding from the whole thalamus showed difference between MTBI patients and controls; with decreased thalamo-thalamo connectivity (red color) and mainly increased thalamo-occipital connectivity (blue color) in MTBI patients compared to controls (minimum $Z>2.3$; cluster significance, $P<0.05$, corrected; cluster size $K\geq100$) with a 25% gray matter mask from the FSL standard template. B: Thalamic segment 4 fcMRI when seed was put in the sub-segment4 (frontal projections) showed more reduced thalamo-thalamo connectivity in red color comparing patients to controls; and similar increased thalamo-occipital connectivity in blue color. C: RS-fcMRI when seed was put in the sub-segment7 (temporal projections) showed thalamic fcMRI differences between MTBI patients and controls with decreased thalamo-thalamo connectivity (red color) while more increased thalamo-cortical connectivity (occipital and scattered frontal white matter regions) in MTBI patients compared to controls.

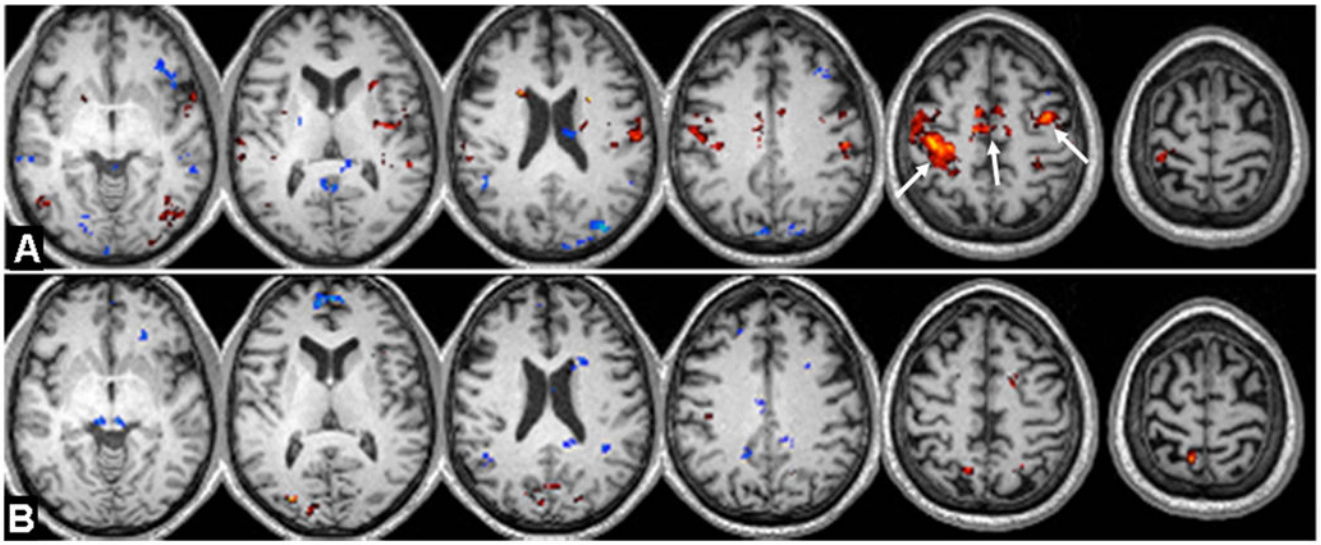

Figure 5.

A: Paired t-test results of comparison between task and RS of the thalamic functional connectivity network during finger tapping task condition in the control group with seed put in the entire thalamus. B: Paired t-test results of comparison of MTBI group-wise thalamic network during finger tapping task condition compared with RS showed less thalamic-task related connectivity (white arrows). Color coded results were thresholded (minimum $Z>2.3$; cluster significance, $P<0.05$, corrected; cluster size $K\geq 20$) based on Gaussian random field theory with a 25% gray matter mask from the FSL standard template.

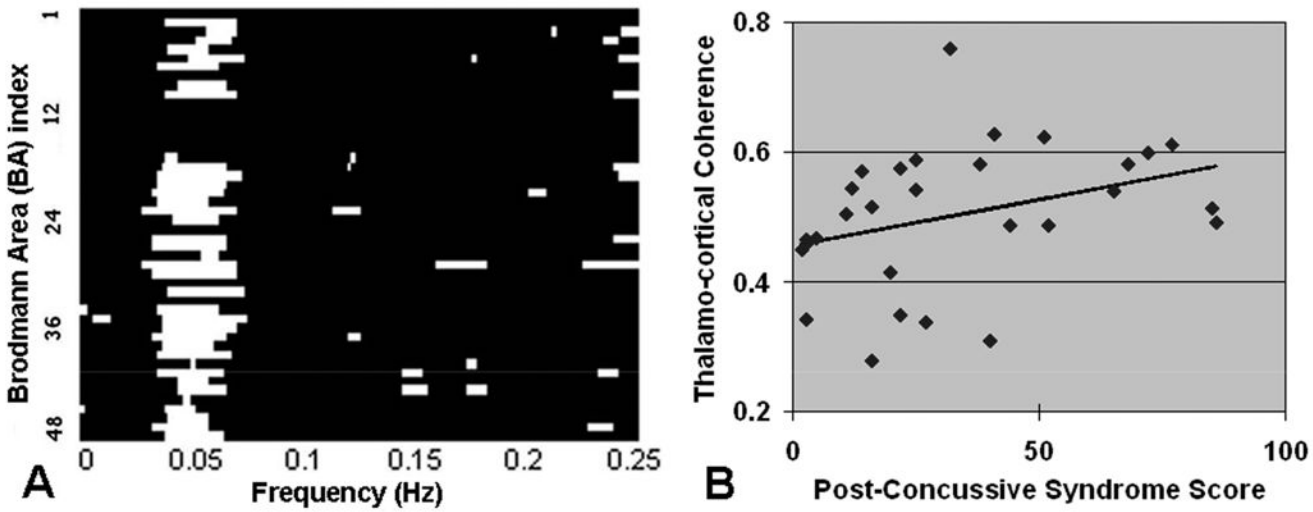

Figure 6.

A: Comparison of coherence between thalamus and cortical regions: there was significantly increased overall coherence between thalamus in MTBI patients compared to controls ($P<0.05$ shown with white bars). Almost all increased thalamo-cortical (BA regions) coherence comes predominantly from low frequency band (0.01-0.08Hz). B: There was positive correlation between low-frequency thalamo-cortical coherence averaged across all cortical BA regions over low-frequency band and post concussive syndrome score (PCS) in MTBI patients (Spearman rank $r=0.4$, $P=0.029$).

Table 1

Statistical differences of fcMRI between MTBI patients and controls with seed regions placed in thalamic segment 4 (cortical frontal projections) bilaterally (P<0.001, cluster-size corrected K≥100).

	Regions	Difference	x,y,z (mm)	K	Z	P
Thalamus	Right	↓	-12,-14,-2	158	3.39	<0.001
Frontal	Left Superior	↓	24,40,56	188	3.79	<0.001
	Right Middle	↓	-46,28,48	136	3.49	<0.001
	Left Middle	↓	16,32,30	65	3.44	<0.001
	Left Insular	↓	24,-12,20	74	3.97	<0.001
Temporal	Right Superior	↓	-38,18,-28	100	3.88	<0.001
	Pole	↓	-50,10,-16	114	3.81	<0.001
Parietal	Right Superior	↑	10,-84,50	504	4.47	<0.001
	Left Lingual	↑	14,-48,-2	85	3.23	0.001
	Right Para-hippocampus	↑	-22,-40,-4	270	3.20	0.001
Occipital	Right Middle	↑	-40,-64,4	768	4.42	<0.001
	Left Middle	↑	36,-62,14	148	4.25	<0.001
	Right Superior	↑	-20,-78,24	88	3.96	<0.001

*↓ denotes decreased connectivity between segment 4 and listed regions in patients compared to controls and ↑ denotes increased connectivity between segment 4 and listed regions in patients compared to controls.

Table 2

Statistical differences of fcMRI between MTBI patients and controls with seed regions placed in thalamic segment 7 (cortical temporal projections) bilaterally (P<0.001, cluster-size corrected K≥100).

Regions		Difference	x,y,z (mm)	K	Z	P
Thalamus	Right	↓	-12,-24,0	243	3.29	0.001
Frontal	Left Inferior	↓	34,36,-14	149	4.47	<0.001
			44,10,8	102	3.54	<0.001
	Right Insular	↓	-26,18,10	200	4.38	<0.001
Temporal	Right Superior Pole	↓	-38,14,-26	238	5.24	<0.001
Frontal	Right Middle	↑	-38,-66,2	153	3.42	<0.001
Parietal	Left Superior	↑	14,-84,52	192	4.23	<0.001
Occipital	Left Cuneus	↑	28,-86,40	103	3.05	0.001
Sub-Cortical	Left Caudate	↑	20,26,2	130	4.57	<0.001

*↓ denotes decreased connectivity between segment 7 and listed regions in patients compared to controls and ↑ denotes increased connectivity between segment 7 and listed regions in patients compared to controls.

Table 3

Summary of significant thalamic fALFF and thalamo-thalamo fcMRI difference (fcMRI at thalamic area seeding from bilateral thalamus and each of its segments) comparing MTBI patients to controls.

Metrics	Whole	Segment1	Segment2	Segment3	Segment4	Segment5	Segment6	Segment7
fALFF	↓	-	-	↓	↓	-	-	↓
fcMRI	↓	-	-	-	↓	-	-	↓

*↓ denotes significant reduction of thalamic fALFF or thalamo-thalamo fcMRI in MTBI patients compared to controls.

*– denotes no significant difference of thalamic fALFF or thalamo-thalamo fcMRI between MTBI patients and controls.

Table 4

Summary of significant cortical fALFF and thalamo-Cortical fcMRI differences comparing MTBI patients to controls.

Metrics		Frontal	Temporal	Parietal	Occipital
fALFF		↓	↓	-	↓
fcMRI	*Whole*	-	↓	-	↑
	Segment 4	↓	↓	↑	↑
	Segment 7	↓	↓	↑	↑

* ↓ denotes decrement and ↑ denotes increment of cortical fALFF or thalamo-cortical fcMRI in MTBI patients compared to controls.

* – denotes no significant difference of cortical fALFF or thalamo-cortical fcMRI between MTBI patients and controls.denotes